Electronic Supplementary Information **(ESI)**

Comparative studies on conventional and solvent-free synthesis toward hydrazones: Application of PXRD and chemometric data analysis in mechanochemical reaction monitoring

Jana Pisk, Tomica Hrenar, Mirta Rubčić, Gordana Pavlović, Vladimir Damjanović, Jasna Lovrić, Marina Cindrić and Višnja Vrdoljak*

Contents

1. Starting compounds and general synthetic route of studied hydrazones

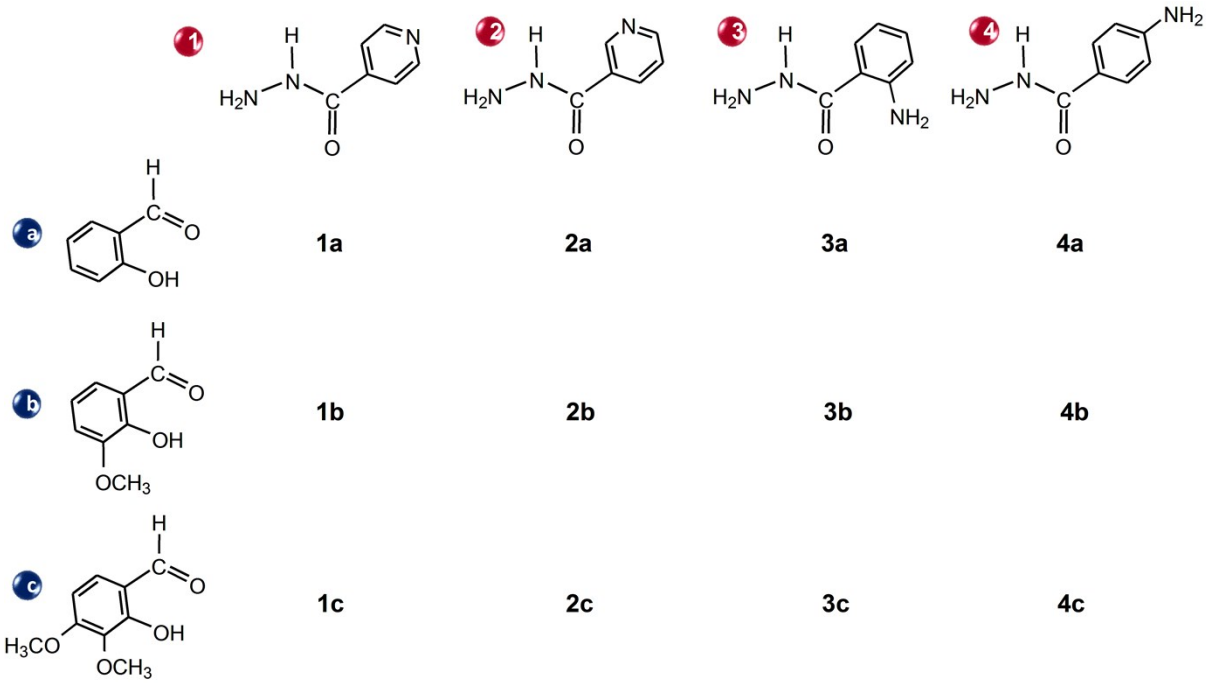

Scheme S1 Aldehydes and hydrazides for hydrazone preparation

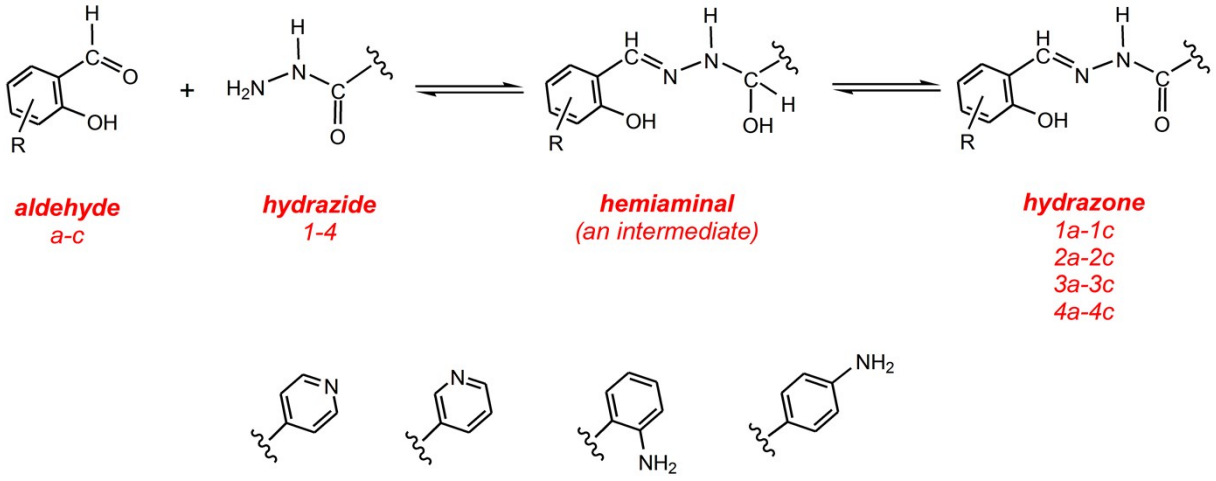

Scheme S2 Equilibrium for the reversible hydrazone formation

2. Tautomeric forms of the hydrazones

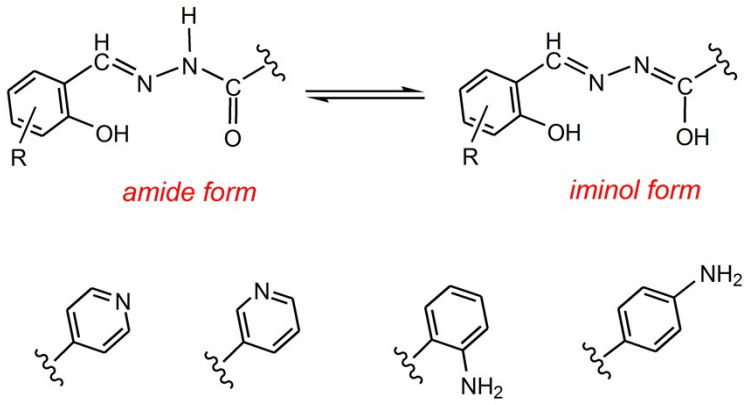

Scheme S3 Tautomerism of the aroylhydrazones

3. Solution based methods

3.1. Solution based synthesis-yields and analytical data

1a was obtained when reaction was performed in methanol. Yield: 0.35 g (29%). Found: C, 64.4; H, 4.3; N, 17.3. $C_{13}H_{11}N_3O_2$ requires C, 64.7; H, 4.6; N, 17.4%. λ_{max}(MeOH)/nm 215 (ε/dm^3 mol^{-1} cm^{-1} 24 700), 292 (17 900) and 335 (15 300). Selected IR data (cm^{-1}): 3252 (N−H), 2835 (H−C)$_{H-C\equiv N}$, 1681 (C=O), 1624 (C=N)py, 1613 (C=N), 1567 (C=C)$_{ring}$, 1272 (C−O), 1160 (N−N).

1b was obtained when reaction was performed in methanol. Yield: 0.96 g (71%). Found: C, 61.85; H, 4.5; N, 15.2. $C_{14}H_{13}N_3O_3$ requires C, 62.0; H, 4.8; N, 15.5%. λ_{max}(MeOH)/nm 222 (ε/dm^3 mol^{-1} cm^{-1} 26 800), 311 (21 900). Selected IR data (cm^{-1}): 3255 (N−H), 2841 (H−C)$_{H-C\equiv N}$, 1690 (C=O), 1627 (C=N)py, 1609 (C=N), 1567(C=C)$_{rin}$g, 1245 (C−O), 1156 (N−N).

1c was obtained when reaction was performed in methanol. Yield: 1.17 g (81%). Found: C, 62.8; H, 4.7; N, 15.35. $C_{14}H_{13}N_3O_3$ requires C, 62.0; H, 4.8; N, 15.5%. λ_{max}(MeOH)/nm 218 (ε/dm^3 mol^{-1} cm^{-1} 22 800) and 337 (22 300). Selected IR data (cm^{-1}): 3252 (N−H), 2835 (H−C)$_{H-C\equiv N}$, 1681 (C=O), 1626 (C=N)py, 1610 (C=N), 1560 (C=C)$_{ring}$, 1274 (C−O), 1122 (N−N).

1c·H$_2$O was obtained when reaction was performed in ethanol. The resulting solution was exposed to atmospheric moisture and left to evaporate slowly at room temperature. Yield: 1.17 g (81%). Found: C, 57.9; H, 5.4; N, 14.25. $C_{14}H_{15}N_3O_4$ requires C, 58.1; H, 5.2; N, 14.5%. Selected IR data (cm^{-1}): 3201 (N−H), 2851 (H−C)$_{H-C\equiv N}$, 1656 (C=O), 1631 (C=N)py, 1609 (C=N), 1550 (C=C)$_{ring}$, 1284 (C−O), 1120 (N−N).

2a-I was obtained when reaction was performed in methanol. The resulting solution was quickly evaporated in vacuo. Yield: 0.66 g (55%). Found: C, 64.5; H, 4.4; N, 17.3. $C_{13}H_{11}N_3O_2$ requires C, 64.7; H, 4.6; N, 17.4%. λ_{max}(MeOH)/nm 215 (ε/dm^3 mol^{-1} cm^{-1} 22 300), 291 (20 500) , 302 (19 500) and 329 (15 400). Selected IR data (cm^{-1}): 3267 (N−H), 2847 (H−C)$_{H-C\equiv N}$, 1681 (C=O), 1624 (C=N)py, 1610 (C=N), 1561 (C=C)$_{ring}$, 1281 (C−O), 1147 (N−N).

2a·H$_2$O was obtained when reaction was performed in ethanol. The resulting solution was exposed to atmospheric moisture and left to evaporate slowly at room temperature. Yield: 0.75 g (58%). Found: C, 60.1; H, 4.9; N, 16.0. $C_{13}H_{13}N_3O_3$ requires C, 60.2; H, 5.1; N, 16.2%. λ_{max}(MeOH)/nm 215 (ε/dm^3 mol^{-1} cm^{-1} 22 300), 291 (20 500), 302 (19 500) and 329 (15 400). Selected IR data (cm^{-1}): 3299 (N−H), 2837 (H−C)$_{H-C\equiv N}$, 1651 (C=O), 1620 (C=N)py, 1610 (C=N), 1556 (C=C)$_{ring}$, 1292 (C−O), 1157 (N−N).

2b·H$_2$O was obtained when reaction was performed in ethanol. Yield: 1.24 g (86%). Found: C, 58.3; H, 5.4; N, 14.2. $C_{14}H_{15}N_3O_4$ requires C, 58.1; H, 5.2; N, 14.5%. λ_{max}(MeOH)/ nm 223 (ε/dm^3 mol^{-1} cm^{-1} 23 300) and 305 (23 400). Selected IR data (cm^{-1}): 3225 (N−H), 2837 (H−C)$_{H-C\equiv N}$, 1672 (C=O), 1627 (C=N)py, 1609 (C=N), 1542 (C=C)$_{ring}$, 1249 (C−O), 1156 (N−N).

2b·MeOH was obtained when reaction was performed in methanol. The resulting solution was slowly evaporated under vacuum at room temperature. Yield: 1.23 g (91%). The solvent molecules escape easily from the crystal. The samples for elemental and TG analysis were completely desolvated until constant weight and were analyzed as **2b**. Found: C, 62.15; H, 5.0; N, 15.2. $C_{14}H_{13}N_3O_3$ requires C, 62.0; H, 4.8; N, 15.5%. λ_{max}(MeOH)/nm 215 (ε/dm^3 mol^{-1} cm^{-1} 22 300), 291 (20 500) , 302 (19 500) and 329 (15 400). Selected IR data (cm^{-1}): 3244 (N−H), 2843 (H−C)$_{H-C\equiv N}$, 1699 (C=O), 1625 (C=N)py, 1609 (C=N), 1554 (C=C)$_{ring}$, 1242 (C−O), 1152 (N−N).

2c·H$_2$O was obtained when reaction was performed in ethanol. The resulting solution was exposed to atmospheric moisture and left to evaporate slowly at room temperature. Yield: 1.36 g (94%). Found: C, 58.3; H, 5.1; N, 14.7. $C_{14}H_{15}N_3O_4$ requires C, 58.1; H, 5.2; N, 14.5%. λ_{max}(MeOH)/ nm

217 (ε/dm^3 mol^{-1} cm^{-1} 20 900) and 333 (24 100). Selected IR data (cm^{-1}): 3227 (N−H), 2844 (H−C)$_{H-C\equiv N}$, 1662 (C=O), 1627 (C=N)py, 1601 (C=N), 1562 (C=C)$_{ring}$, 1246 (C−O), 1166 (N−N).

2c·MeOH was obtained when reaction performed in methanol. The resulting solution was slowly evaporated under vacuum at room temperature. Yield: 0.93 g (69%). The solvent molecules escape easily from the crystal. This solid turns into white powder upon standing at room temperature. The samples for elemental and TG analysis were completely desolvated until constant weight and were analyzed as **2c**. Found: C, 62.25; H, 5.0; N, 15.2. $C_{14}H_{13}N_3O_3$ requires C, 62.0; H, 4.8; N, 15.5Selected IR data (cm^{-1}): 3202 (N−H), 2845 (H−C)$_{H-C\equiv N}$, 1646 (C=O), 1627 (C=N)py, 1601 (C=N), 1576 (C=C)$_{ring}$, 1224 (C−O), 1167 (N−N).

3a was obtained when reaction was performed in methanol. Yield: 1.12 g (87%). Found: C, 65.7; H, 5.3; N, 16.3. $C_{14}H_{13}N_3O_2$ requires C, 65.9; H, 5.1; N, 16.5%. λ_{max}(MeOH)/ nm 218 (ε/dm^3 mol^{-1} cm^{-1} 25 800), 288 (14 400) , 298 (14 500) and 342 (11 800). Selected IR data (cm^{-1}): 3270 (N−H), 2836 (H−C)$_{H-C\equiv N}$, 1657 (C=O), 1610 (C=N), 1583 (C=C)$_{ring}$, 1244 (C−O), 1147 (N−N).

3b was obtained when reaction was performed in methanol. Yield: 1.28 g (88%). Found: C, 63.3; H, 5.4; N, 14.5. $C_{15}H_{15}N_3O_3$ requires C, 63.1; H, 5.3; N, 14.7%. λ_{max}(MeOH)/ nm 223 (ε/dm^3 mol^{-1} cm^{-1} 33 300), 304 (21 800) and 348 (15 900). Selected IR data (cm^{-1}): 3262 (N−H), 2833 (H−C)$_{H-C\equiv N}$, 1642 (C=O), 1610 (C=N), 1588 (C=C)$_{ring}$, 1244 (C−O), 1151 (N−N).

3c was obtained when reaction was performed in methanol. Yield: 1.12 g (77%). Yield Found: C, 62.9; H, 5.2; N, 14.85. $C_{15}H_{15}N_3O_3$ requires C, 63.1; H, 5.3; N, 14.7%. %. λ_{max}(MeOH)/ nm 220 (ε/dm^3 mol^{-1} cm^{-1} 30 000), 331 (22 800) and 346 (24 100). Selected IR data (cm^{-1}): 3270 (N−H), 2838 (H−C)$_{H-C\equiv N}$, 1631 (C=O), 1609 (C=N), 1587 (C=C)$_{ring}$, 1245 (C−O), 1162 (N−N).

4a was obtained when reaction was performed in methanol. Yield: 1.06 g (78%). Found: C, 63.1; H, 5.4; N, 7.2. $C_{14}H_{13}N_3O_2$ requires C, 65.9; H, 5.1; N, 16.5%. λ_{max}(MeOH)/ nm 228 (ε/dm^3 mol^{-1} cm^{-1} 19 500) and 333 (33 100). Selected IR data (cm^{-1}): 3276 (N−H), 2857 (H−C)$_{H-C\equiv N}$, 1653 (C=O), 1620 (C=N), 1599 (C=C)$_{ring}$, 1259 (C−O), 1153 (N−N).

4b was obtained when reaction was performed in methanol. The resulting solution was quickly evaporated in vacuo. Yield: 1.12 g (77%). Found: C, 63.1; H, 5.4; N, 7.2. $C_{15}H_{15}N_3O_3$ requires C, 63.1; H, 5.3; N, 14.7%. λ_{max}(MeOH)/ nm 222 (ε/dm^3 mol^{-1} cm^{-1} 23 900) and 321 (34 800). Selected IR data (cm^{-1}): 3218 (N−H), 2841 (H−C)$_{H-C\equiv N}$, 1653 (C=O), 1620 (C=N), 1599 (C=C)$_{ring}$, 1259 (C−O), 1162 (N−N).

4b·MeOH was obtained when reaction was performed in methanol. The resulting solution was slowly evaporated under vacuum at room temperature. Yield: 0.62 g (42%). The solvent molecules escape easily from the crystal. The samples for elemental and TG analysis were completely desolvated until constant weight and were analyzed as **4b**. Found: C, 63.3; H, 5.4; N, 14.5. $C_{15}H_{15}N_3O_3$ requires C, 63.1; H, 5.3; N, 14.7%. λ_{max}(MeOH)/ nm 222 (ε/dm^3 mol^{-1} cm^{-1} 23 900) and 321 (34 800). Selected IR data (cm^{-1}): 3218 (N−H), 2863 (H−C)$_{H-C\equiv N}$, 1658 (C=O), 1619 (C=N), 1600 (C=C)$_{ring}$, 1260 (C−O), 1178 (N−N).

4b·EtOH was obtained when reaction was performed in ethanol. The resulting solution was slowly evaporated under vacuum at room temperature. Yield: 0.96 g (66%). Crystals lose solvated molecules on prolonged standing at room temperature and were analyzed as **4b**. Found: C, 63.3; H, 5.55; N, 14.45. $C_{15}H_{15}N_3O_3$ requires C, 63.1; H, 5.3; N, 14.7%. λ_{max}(MeOH)/ nm 222 (ε/dm^3 mol^{-1} cm^{-1} 23 900) and 321 (34 800). Selected IR data (cm^{-1}): 3218 (N−H), 2867 (H−C)$_{H-C\equiv N}$, 1655 (C=O), 1619 (C=N), 1599 (C=C)$_{ring}$, 1259 (C−O), 1153 (N−N).

4c was obtained when reaction was performed in methanol. Yield: 1.08 g (74%). Found: C, 63.1; H, 5.4; N, 7.2. $C_{15}H_{15}N_3O_3$ requires C, 63.1; H, 5.3; N, 14.7%. λ_{max}(MeOH)/ nm 336 (ε/dm^3 mol^{-1} cm^{-1} 44 600). Selected IR data (cm^{-1}): 3212 (N−H), 2839 (H−C)$_{H-C\equiv N}$, 1634 (C=O), 1625 (C=N), 1599 (C=C)$_{ring}$, 1276 (C−O), 1164 (N−N).

3.2. Crystalization conditions and analytical data

Table S1. Crystallization conditions and resulting crystal forms

Compound	MeOH	EtOH	1-PrOH	Ethyl acetate	MeCN	Acetone
1a	+	+	+	+	+	+
1b	+	+	+	+	+	+
1c	+	–	–	–	–	–
1c·H_2O	+	+	+	+	+	+
2a-I	+	–	+	–	–	–
2a-II	–	+	–	–	+	+
2a·H_2O	+	+	–	+	–	–
2b	–	–	–	–	–	–
2b·H_2O	+	+	+	+	+	+
2b·MeOH	+	–	–	–	–	–
2c-I	–	–	–	–	–	–
2c-II	–	–	–	–	–	–
2c·H_2O	–	+	+	+	*	+
2c·MeOH	+	–	–	–	–	–
3a	+	+	+	+	+	+
3b	+	+	+	+	+	+
3c	+	+	+	+	+	+
4a	+	+	+	+	+	+
4b	+	–	–	–	–	–
4b·MeOH	+	–	–	–	–	–
4b·EtOH	–	+	–	–	–	–
4a·H_2O	–	–	+	+	+	+
4c	+	+	+	+	+	+

* mixture

2a-II Found: C, 64.4; H, 4.3; N, 17.5. $C_{13}H_{11}N_3O_2$ requires C, 64.7; H, 4.6; N, 17.4%. λ_{max}(MeOH)/nm 215 (ε/dm^3 mol^{-1} cm^{-1} 22 300), 291 (20 500), 302 (19 500) and 329 (15 400). Selected IR data (cm^{-1}): 3312 (N−H), 2862 (H−C)$_{H-C=N}$, 1668 (C=O), 1623 (C=N)py, 1610 (C=N), 1603 (C=C)$_{ring}$, 1271 (C−O), 1155 (N−N).

4b·H_2O. Found: C, 59.1; H, 5.4; N, 14.2. $C_{15}H_{17}N_3O_4$ requires C, 59.4; H, 5.6; N, 13.85%. λ_{max}(MeOH)/ nm 228 (ε/dm^3 mol^{-1} cm^{-1} 19 500) and 333 (33 100). Selected IR data (cm^{-1}): 3276 (N−H), 2866 (H−C)$_{H-C=N}$, 1640 (C=O), 1625 (C=N), 1603 (C=C)$_{ring}$, 1271 (C−O), 1155 (N−N).

4. Solution based synthesis - Powder X-ray diffraction patterns

4.1. PXRD patterns of the isonicotinic hydrazide based hydrazones

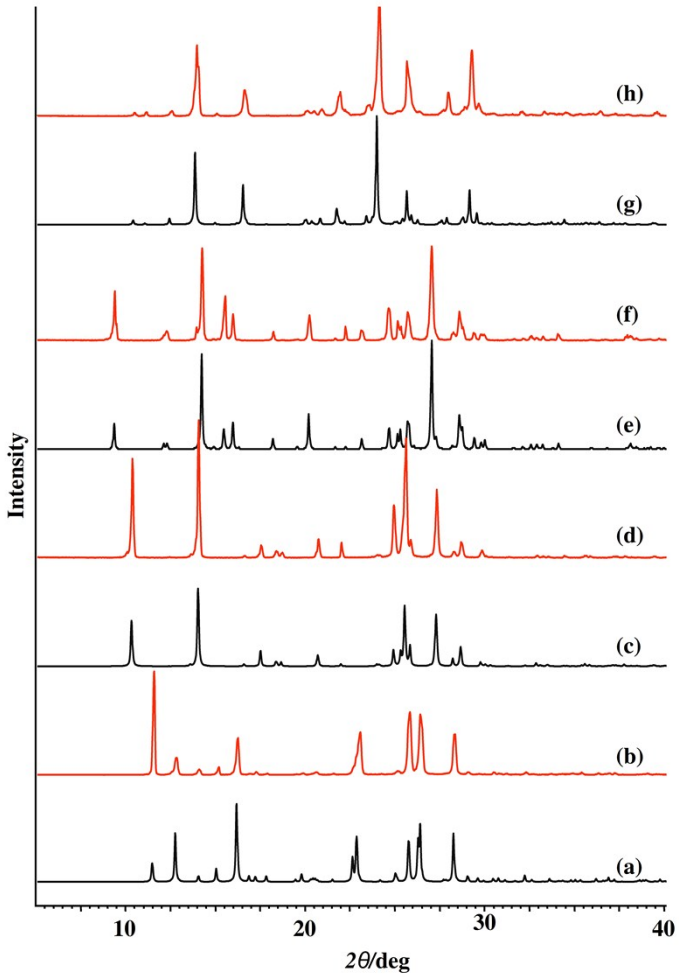

Fig. S1 PXRD patterns of the isonicotinic hydrazide based hydrazones: (a) **1a** calculated from the single-crystal structure, refcode: WEHFEU; (b) **1a** obtained by the solution based method; (c) **1b** calculated from the single-crystal structure, refcode: CANCOK; (d) **1b** obtained by the solution based method; (e) **1c·H_2O** calculated from the single-crystal structure, refcode: ROFXOA; (f) **1c ·H_2O** obtained by the solution based method; (g) **1c** calculated from the single-crystal structure, refcode: KUTPOF and (h) **1c** obtained by the solution based method.

4.2. PXRD patterns of the nicotinic hydrazide based hydrazones

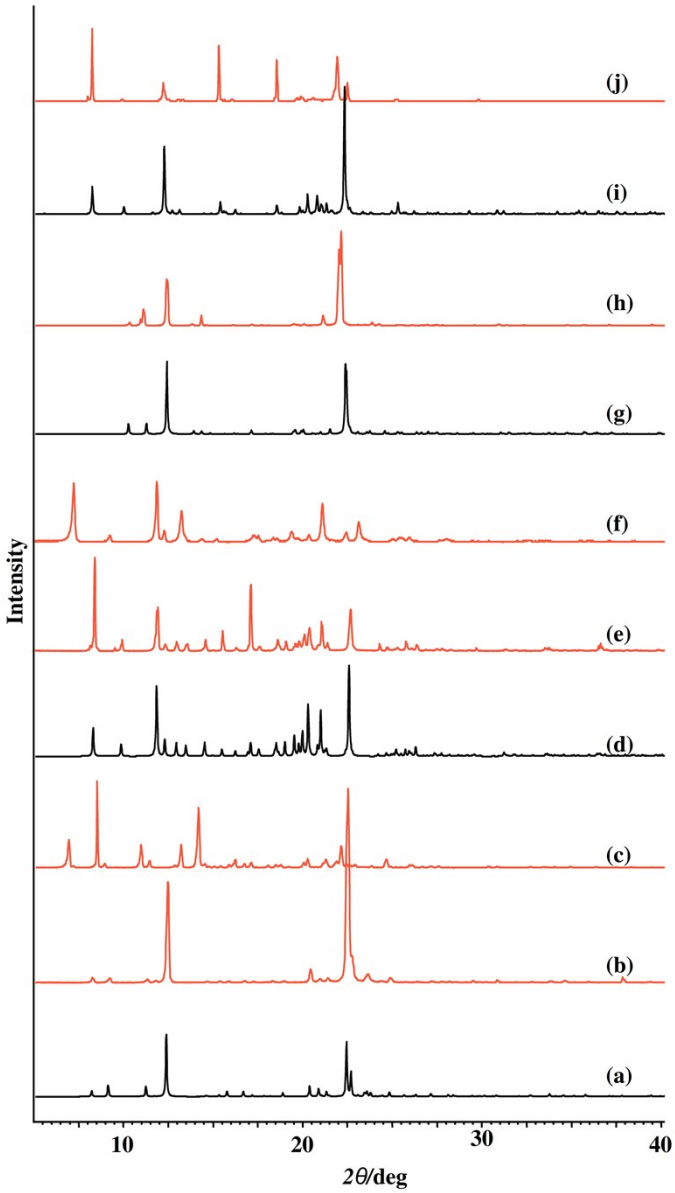

Fig. S2 PXRD patterns of the nicotinic hydrazide based hydrazones: (a) **2a·H_2O** calculated from the single-crystal structure, refcode: IDASUB; (b) **2a·H_2O** obtained by the solution based method; (c) **2a** obtained by the solution based method; (d) **2b·MeOH** calculated from the X-ray single-crystal structure; (e) **2b·MeOH** obtained by the solution based method; (f) **2b·H_2O** obtained by the solution based method; (g) **2c·H_2O** calculated from the single-crystal structure, refcode: XIBZOY, (e) **2c·H_2O** obtained by the solution based method; (i) **2c·MeOH** calculated from the X-ray single-crystal structure and (j) **2c·MeOH** obtained by the solution based method.

4.3. PXRD patterns of the 2-aminobenzhydrazide based hydrazones

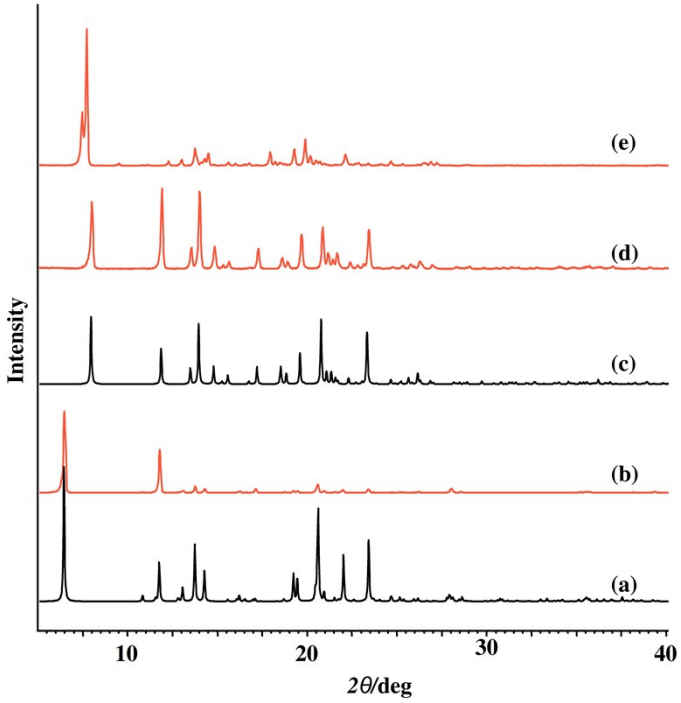

Fig. S3 PXRD patterns of 2-aminobenzhydrazide based hydrazones: (a) **3a** calculated from the single-crystal structure, refcode: MUNDUU; (b) **3a** obtained by the solution based method; (c) **3b** calculated from the X-ray single-crystal structure; (d) **3b** obtained by the solution based method and (e) **3c** obtained by solution based method.

4.3. PXRD patterns of the 4-aminobenzhydrazide based hydrazones

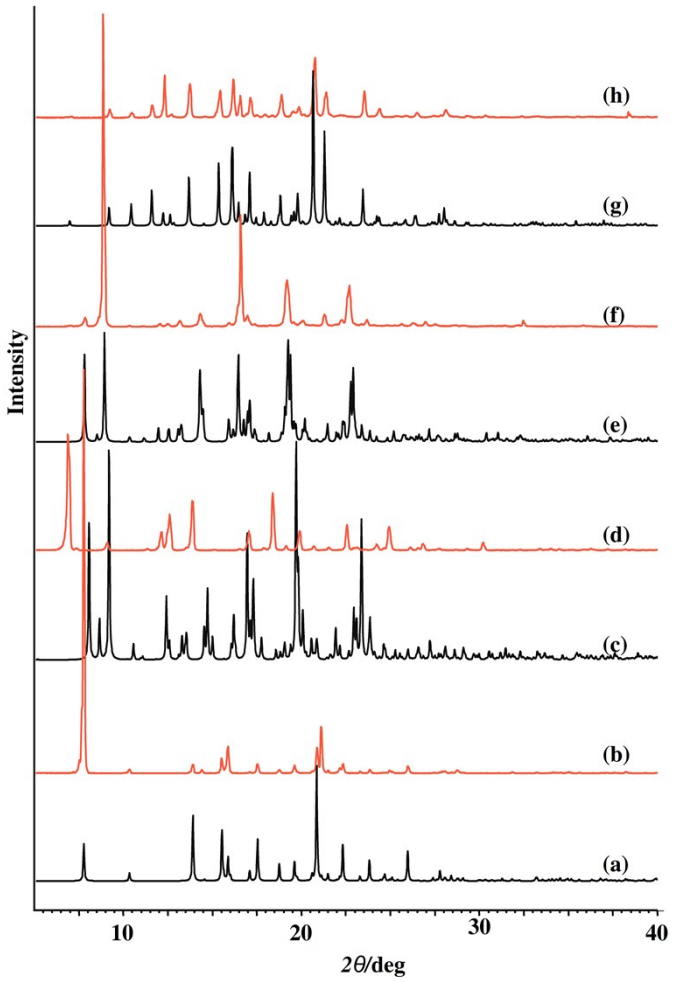

Fig. S4 PXRD patterns of the 4-aminobenzhydrazide based hydrazones: (a) **4a** calculated from the single-crystal structure; (b) **4a** obtained by the solution based method; (c) **4b·MeOH** calculated from the single-crystal structure; (d) **4b·MeOH** obtained by the solution based method; (e) **4b·EtOH** calculated from the X-ray single-crystal structure; (f) **4b·EtOH** obtained by the solution based method; (g) **4c** calculated from the X-ray single-crystal structure and (h) **4c** obtained by the solution based method.

5. Solid state transformations of the solvated forms - Powder X-ray diffraction patterns

5.1. Powder X-ray diffraction patterns of the alcohol solvate forms

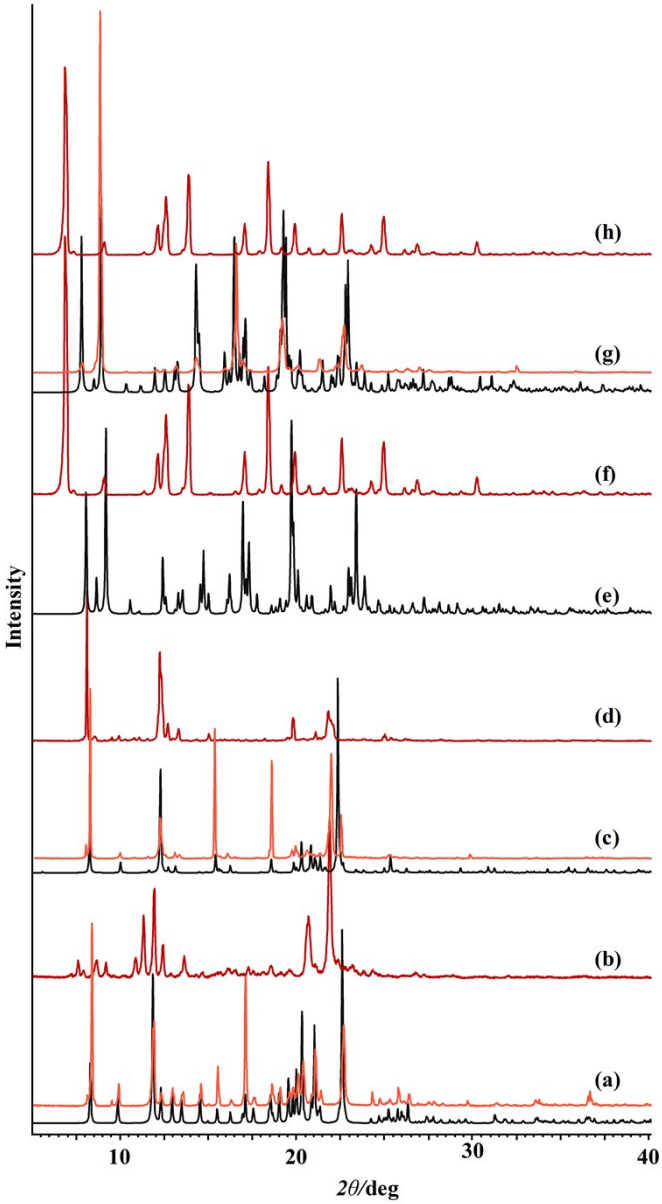

Fig. S5 Powder X-ray diffraction patterns of the alcohol solvate forms obtained by the solution based method (the dark orange lines), simulated patterns (black lines) and unsolvated species (the red lines) of (a) **2b·MeOH** ; (b) **2b** obtained upon desolvation of **2b·MeOH**; (c) **2c·MeOH**; (d) **2c** obtained upon desolvation of **2c·MeOH**; (e) **4b·MeOH**; (f) **4b** obtained upon desolvation of **4b·MeOH**; (g) **4b·EtOH**; (h) **4b** obtained upon desolvation of **4b·EtOH.**

5.2. Powder X-ray diffraction patterns of the hydrate forms

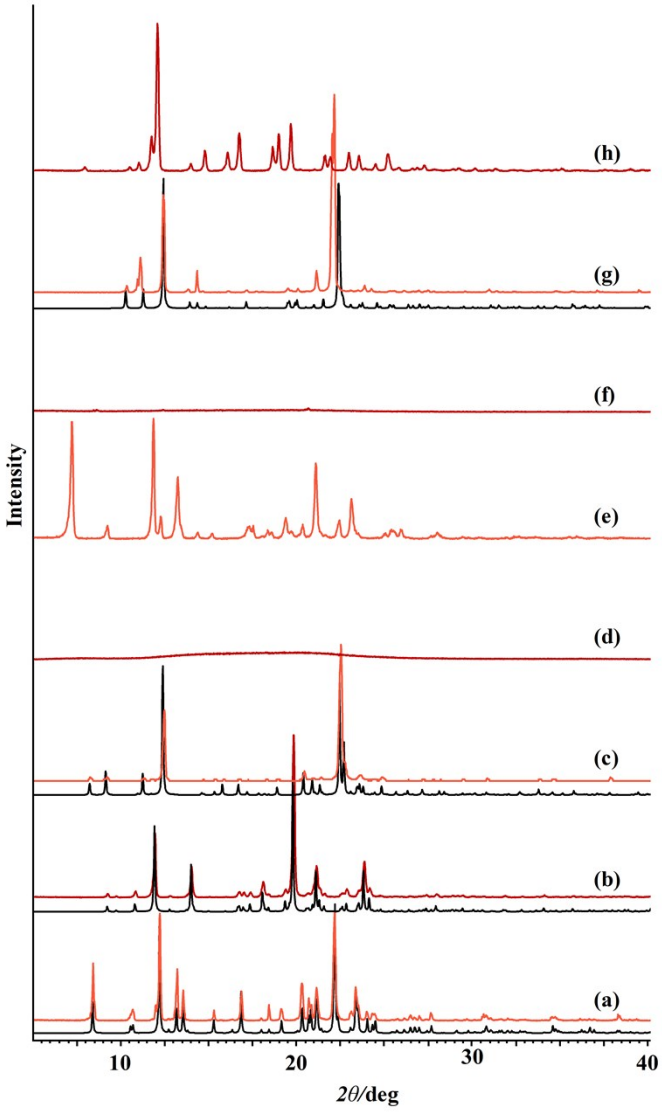

Fig. S6 Powder X-ray diffraction patterns of the hydrate forms obtained by the solution based method (the dark orange lines), simulated patterns (black lines) and anhydrous forms (the red lines) of (a) **1c·H_2O**; refcode REFXOA (b) **1c** obtained upon heating of **1c**·H_2O in the O_2 atmosphere at 200 °C for 1 h; refcode KUTPOF; (c) **2a·H_2O**; refcode IDASUB (d) **2a** obtained upon heating of **2a·H_2O** in the O_2 atmosphere at 170 °C for 1 h; (e) **2b·H_2O**; (f) **2b** obtained upon heating of **2b·H_2**O in the O_2 atmosphere at 110 °C for 1 h; (g) **2c·H_2O**; refcode XIBZOY (h) **2c** obtained upon heating of **2c·H_2O** in the O_2 atmosphere at 150 °C for 1 h.

6. Application of PXRD and Chemometric Data Analysis in Reaction Monitoring

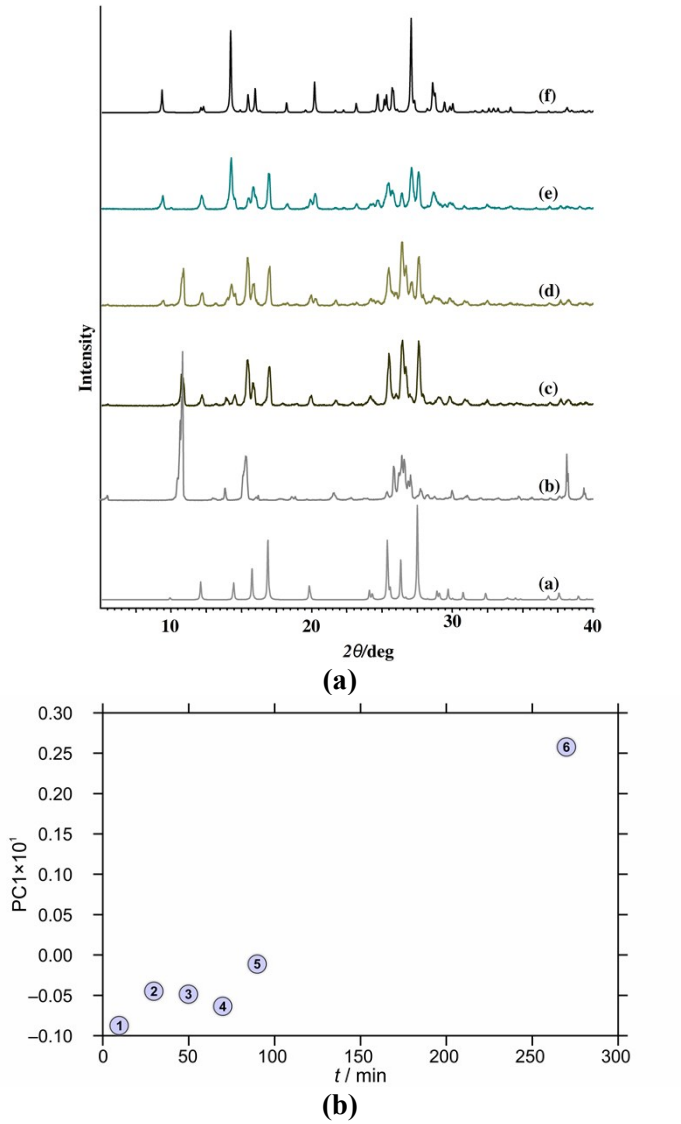

Fig. S7 (a) Comparison of PXRD patterns between the starting materials and appearance of the products as a function of time (a) PXRD patterns of isonicotinic hydrazide calculated from the deposited crystal structure (refcode: INICAC); (b) PXRD patterns of 4-methoxysalicyladehyde; *Ex-situ* X-ray diffraction analysis at room temperature of the 1:1 reaction between 4-methoxysalicyladehyde and isonicotinic hydrazide after (c) 10 min; (d) 90 min; (e) 270 min and (f) PXRD patterns of **1c** calculated from the deposited crystal structure (refcode: ROFXOA). **(b)** Time dependence of PC1 scores calculated for a set of PXRD data collected through mechanochemical synthesis of **1c**.

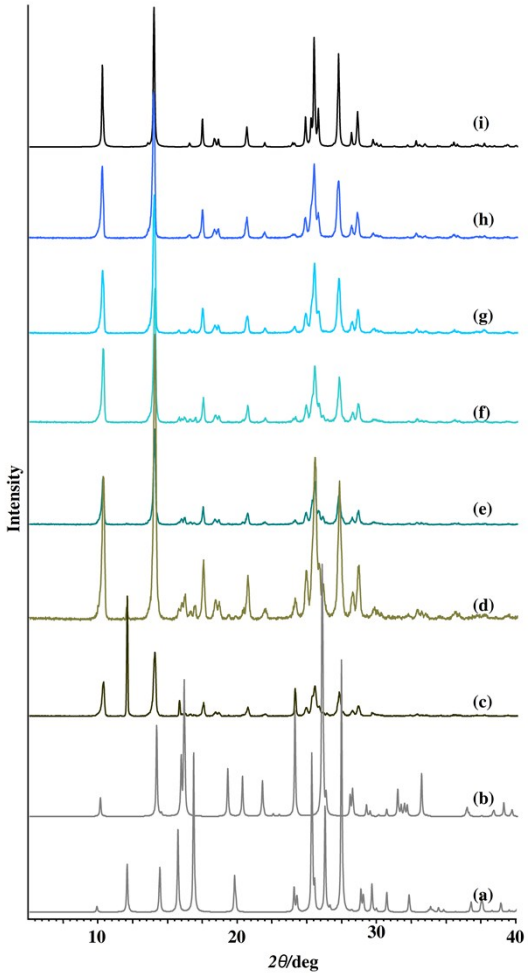

(a)

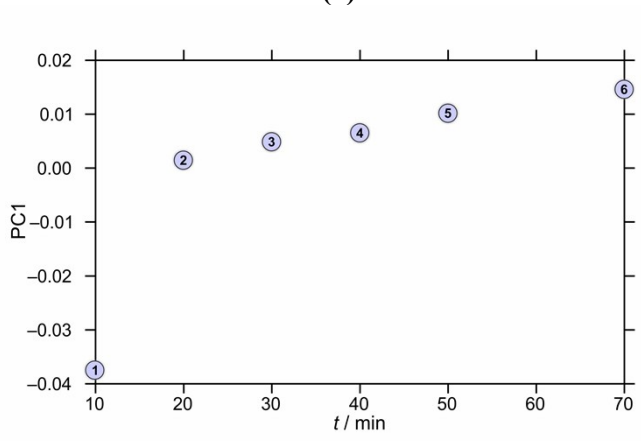

(b)

Fig. S8 (a) Comparison of PXRD patterns between the starting materials and appearance of the products as a function of time (a) PXRD patterns of isonicotinic hydrazide calculated from the deposited crystal structure (refcode: INICAC); (b) PXRD patterns of 3-methoxysalicylaldehyde calculated from the deposited crystal structure (refcode: OVANIL); *Ex-situ* X-ray diffraction analysis at room temperature of the 1:1 reaction between 3-methoxysalicylaldehyde and isonicotinic hydrazide after (c) 10 min; (d) 20 min; (e) 30 min; (f) 40 min; (g) 50 min; (h) 70 min and (i) PXRD patterns of **1b** calculated from the deposited crystal structure (refcode: CANCOK). **(b)** Time dependence of PC1 scores calculated for a set of PXRD data collected through mechanochemical synthesis of **1b**.

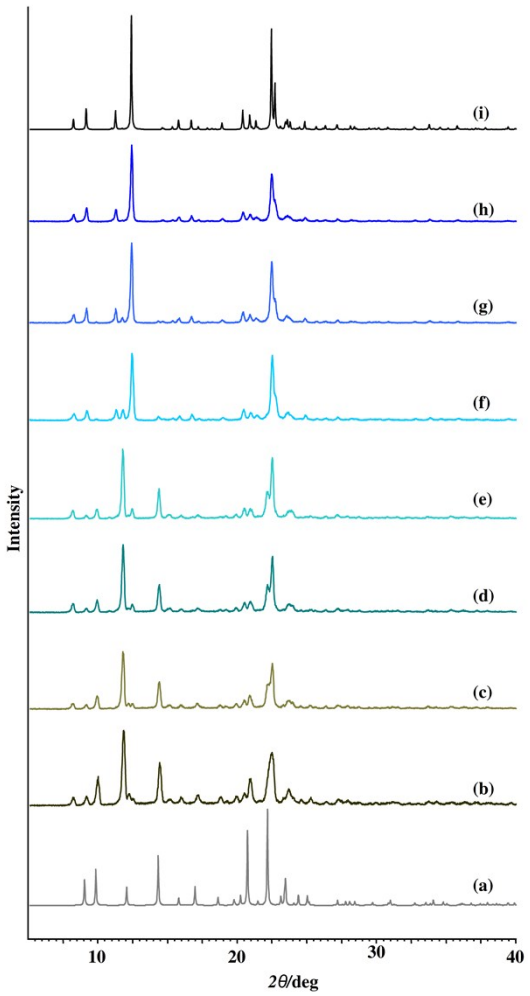

(a)

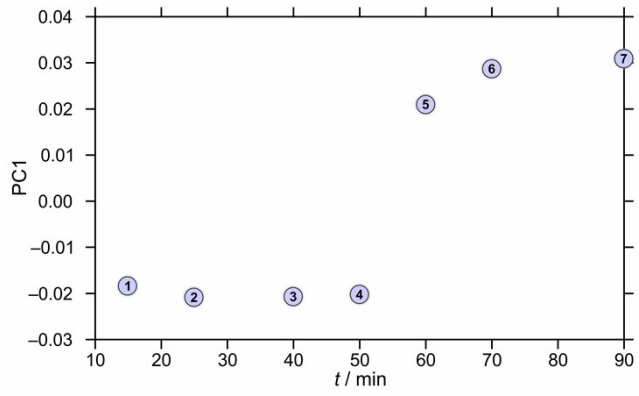

(b)

Fig. S9 (a) Comparison of PXRD patterns between the starting materials and appearance of the products as a function of time (a) PXRD patterns of nicotinic hydrazide calculated from the deposited crystal structure (refcode: GIRYEM); *Ex-situ* X-ray diffraction analysis at room temperature of the 1:1 reaction between salicylaldehyde and nicotinic hydrazide after (b) 15 min; (c) 25 min; (d) 40 min; (e) 50 min; (f) 60 min; (g) 70 min; (h) 90 min and (i) PXRD patterns of **2a·H_2O** calculated from the deposited crystal structure (refcode: IDASUB). **(b)** Time dependence of PC1 scores calculated for a set of PXRD data collected through mechanochemical synthesis of **2a·H_2O**

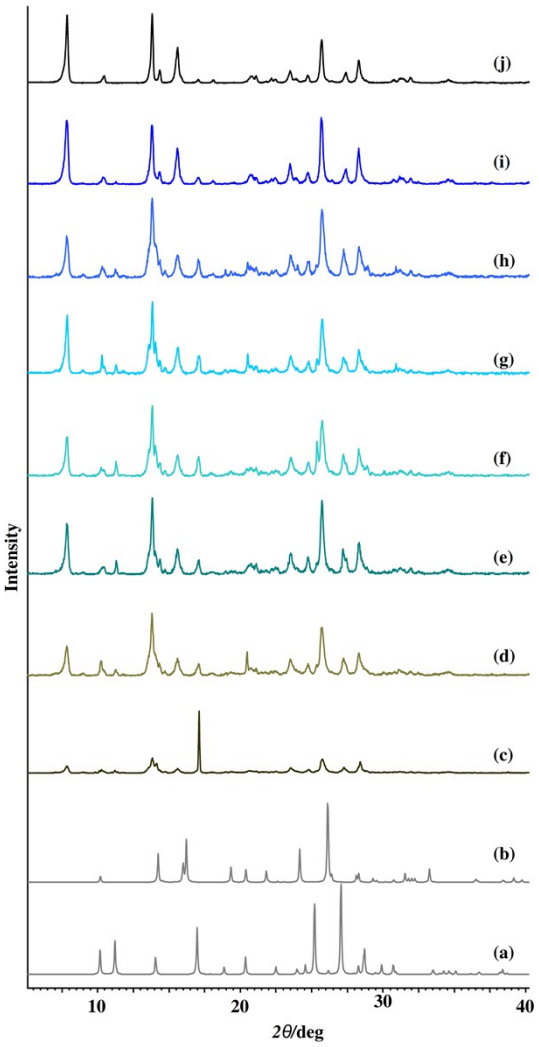

(a)

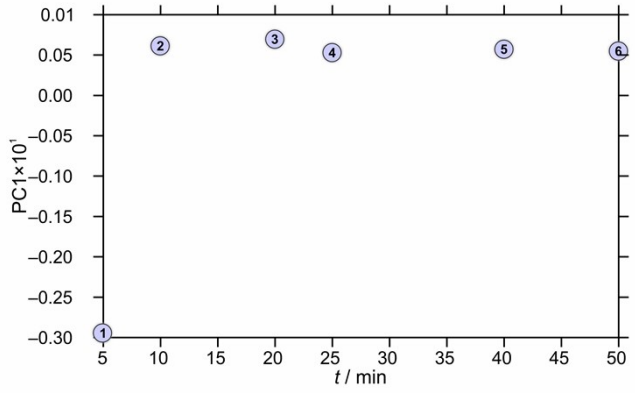

(b)

Fig. S10 (a) Comparison of PXRD patterns between the starting materials and appearance of the products as a function of time (a) PXRD patterns of nicotinic hydrazide calculated from the deposited crystal structure (refcode: GIRYEM); (b) PXRD patterns of 3-methoxysalicylaldehyde calculated from the deposited crystal structure (refcode: OVANIL); *Ex-situ* X-ray diffraction analysis at room temperature of the 1:1 reaction between 3-methoxysalicylaldehyde and nicotinic hydrazide after (c) 5 min; (d) 10 min; (e) 20 min; (f) 25 min; (g) 40 min; (h) 50 min; (i) 70 min and (j) PXRD patterns of **2b·H_2O** of the sample obtained by solution based method. **(b)** Time dependence of PC1 scores calculated for a set of PXRD data collected through mechanochemical synthesis of **2b·H_2O**.

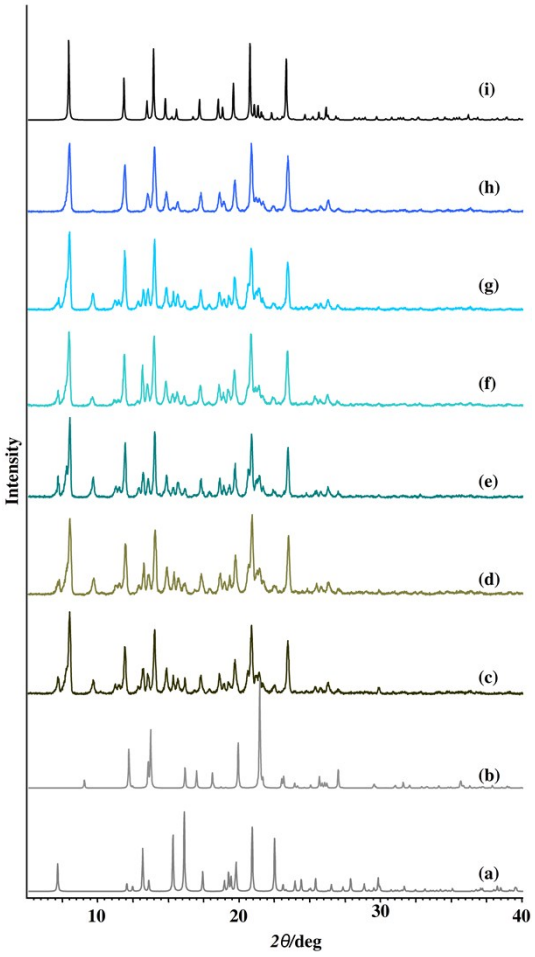

(a)

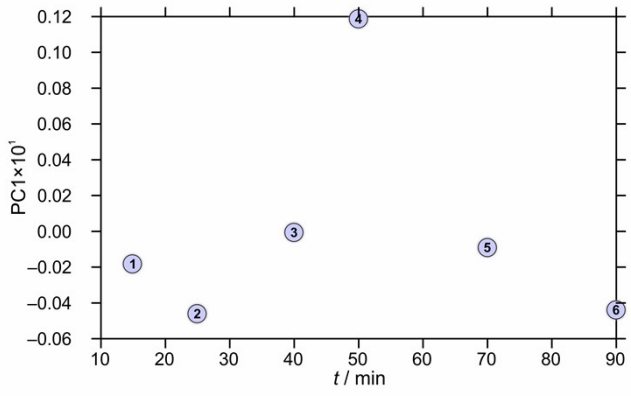

(b)

Fig. S11 (a) Comparison of PXRD patterns between the starting materials and appearance of the products as a function of time (a) PXRD patterns of 2-aminobenzhydrazide calculated from the deposited crystal structure (refcode: CEDREJ); (b) PXRD patterns of 3-methoxysalicylaldehyde calculated from the deposited crystal structure (refcode: OVANIL); *Ex-situ* X-ray diffraction analysis at room temperature of the 1:1 reaction between 3-methoxysalicylaldehyde and 2-aminobenzhydrazide after (c) 15 min; (d) 25 min; (e) 40 min; (f) 50 min; (g) 70 min; (h) 90 min and (i) PXRD patterns of **3b** calculated from the X-ray single-crystal structure. **(b)** Time dependence of PC1 scores calculated for a set of PXRD data collected through mechanochemical synthesis of **3b**.

7. X-Ray Crystallography. Single crystal diffraction.

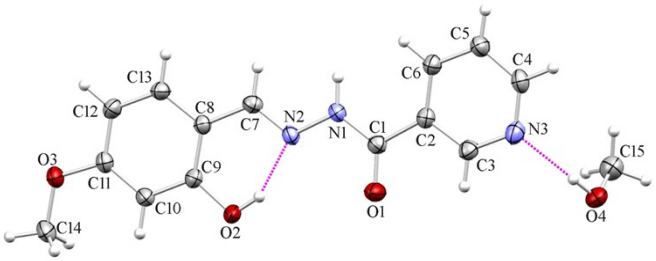

Fig. S12 Mercury-POV-Ray drawing of the asymmetric units of **2c·MeOH**. The displacement ellipsoids are drawn at the 50 % probability level at 296(2) K. The hydrogen atoms are drawn as spheres of arbitrary radius. Intramolecular hydrogen bonds within asymmetric unit are shown as pink dashed lines.

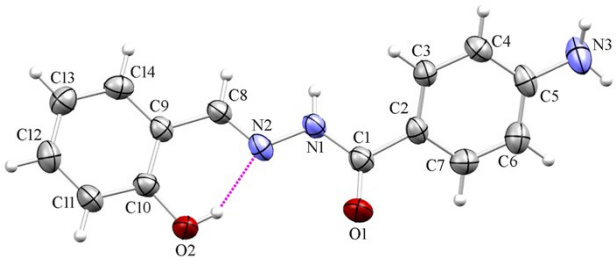

Fig. S13 Mercury-POV-Ray drawing of the asymmetric units of **4a**. The displacement ellipsoids are drawn at the 50 % probability level at 296(2) K. The hydrogen atoms are drawn as spheres of arbitrary radius. Intramolecular hydrogen bonds within asymmetric unit are shown as pink dashed lines.

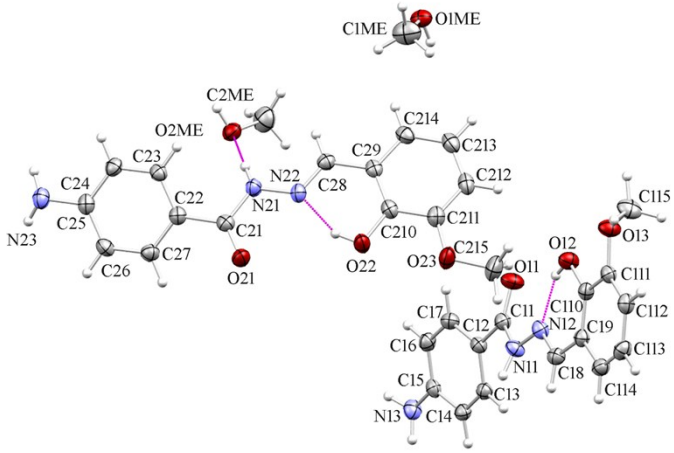

(a)

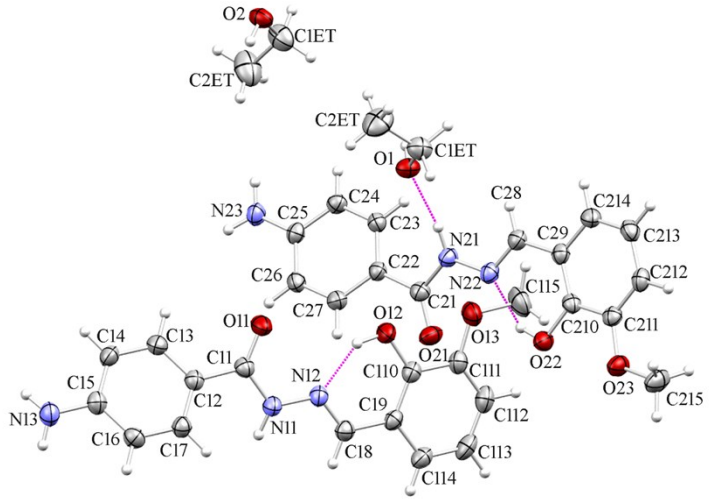

(b)

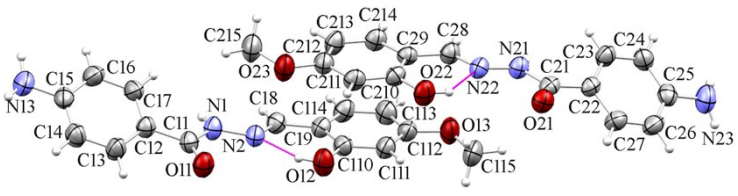

(c)

Fig. S14 Mercury-POV-Ray drawing of the asymmetric units of **4b·MeOH**, **4b·EtOH** and **4c**. The displacement ellipsoids are drawn at the 50 % probability level at 296(2) K for **4c** and 150(2) K for **4b·MeOH** and **4b·EtOH**. The hydrogen atoms are drawn as spheres of arbitrary radius. Intramolecular hydrogen bonds within asymmetric unit are shown as pink dashed lines.

7. 1. Description of supramolecular architectures

Nicotinic hydrazide derivatives. The molecules of **2b·MeOH** (Fig. S15) and **2c·MeOH** (Fig. 9) are assembled into infinite $C\frac{2}{2}$ chains formed *via* two discrete motifs N1···O4 and O4···N3 intermolecular hydrogen bonds between the amide –NH group and the O4 atom from methanol molecule and between the O4 atom and the pyridine N3 atom. The fused hydrogen bonded rings of the type $\mathrm{R}\frac{1}{2}(7)\mathrm{R}\frac{1}{2}(6)$ are formed via C–H···O type of hydrogen bonds including C7···O4 and C6···O4, in both structures. These two supramolecular synthons form $\mathrm{R}\frac{1}{3}(9)$ puckered ring.

In **2b·MeOH** there is additional $R\frac{2}{2}(12)$ ring formed *via* C13–H13···O1 intermolecular hydrogen bond with the O1 carbonyl oxygen atom as proton acceptor (Fig. 9). In that way, three fused rings are formed into 2D infinite chain of $R\frac{2}{3}(16)$ rings. In **2c·MeOH** structure (Fig. 9) the carbonyl O1 atom and the hydroxyl O2 atom forms very weak intermolecular hydrogen bond with the methyl C15 methanol (Table S4) forming the new type puckered ring described as $R\frac{3}{3}(9)$ supramolecular synthon, unlike in **2b·MeOH**. In both structures, the methanol O4 atom acts as a trifurcated proton acceptor and simultaneously proton donor. The methoxy O3 atom participates into very weak, but different hydrogen bond formation C4–H4···O3 and C15–H15C···O3 in **2b·MeOH** and **2c·MeOH**, respectively. The participation of the methoxy O3 atom in formation of different hydrogen bonds is probably caused by different positions on phenyl ring in **2b·MeOH** and **2c·MeOH**, respectively. The carbonyl O1 atom also forms different hydrogen bonds in **2b·MeOH** and **2c·MeOH**, respectively. While in **2b·MeOH** the O1 atom forms two hydrogen bonds with Car–H and C_{sp3}–H methyl methoxy group (C13–H13···O1 and C14–H14B···O1, respectively), in **2c·MeOH** it forms hydrogen bond with methyl methanol group (C15–H15A···O1).

2-Aminobenzhydrazide derivatives. In **3b** two discrete motifs described by graph-set notations as *S*(6) exist: O2–H12O···N2 intramolecular hydrogen bond between hydroxyl O2 atom and N2 and N3–H13N···O1 between amine group and carbonyl O1 atom (Table S4, Fig. 10). The carbonyl O1 atom is bifurcated as proton acceptor between hydrogen atoms of amine group. This bifurcation enables formation of $C\frac{1}{2}(4)$ infinite chains based on two hydrogen bonds: intra N3–H13N···O1 and inter N3–H23N···O1 hydrogen bond.

Taking into consideration weak C–H···O intermolecular hydrogen bonds; bifurcation at hydroxyl O2 atom occurs with C_{ar}–H groups (C13–H13···O2 and C14–H14···O2

intermolecular hydrogen bonds) forming planar five-membered hydrogen bonded ring denoted as $R\frac{1}{2}(5)$. Simultaneously, C13–H13 group is bifurcated between hydroxyl O2 and methoxy O3 atom forming $R\frac{2}{1}(5)$ supramolecular synthon. Both these rings are fused into new $R\frac{2}{2}(8)$ synthon.

4-Aminobenzhydrazide derivatives. The hydroxyl O2 atom acts simultaneously as proton donor in *S*(6) intramolecular hydrogen bond (O2–H12O···N2) and as proton acceptor in N1–H1···O2 intermolecular hydrogen bond in **4a** (Fig. 11). The carbonyl O1 is bifurcated between amine N3 atom (N3–H23N···O1) and C_{ar}–H group of another molecule (C14–H14···O1) forming two intermolecular hydrogen bonds (Table S4). In that way, 3D hydrogen bonded network is shaped.

The crystal structures of **4b·EtOH** (Fig. 12) and **4b·MeOH** (Fig S16) are analogous at the level of strong and moderate hydrogen bonds, but there is a difference considering weak C–H···O (C_{ar}–H···O and C_{sp3}–H···O) type of hydrogen bonds formed with the hydroxyl oxygen atom O12 (Table S4).

The crystal structure of **4b·EtOH** is dominated by hydrogen bonds between two symmetrically dependent molecules (Fig. 12). The hydroxyl oxygen atom acts as proton donor in *S*(6) intramolecular hydrogen bond with nitrogen atom. The amide nitrogen atoms with carbonyl oxygen atoms are linked *via* ethanol O2 atom which acts simultaneously as proton donor O2–H11···O11 and double proton acceptor forming two hydrogen bonds with amide and amine nitrogen atoms (N11–H11N···O2 and N13–H13N···O2) (Table S4). In such a way, the molecular layers of symmetrically dependent molecules are crosslinked *via* hydrogen bonds with ethanol molecule (Fig. S17 (b)). The symmetrically independent molecules are joined weakly *via* C_{sp3}-H···O(hydroxyl) intermolecular hydrogen bonds (Table S4).

Another amine group hydrogen atom is bifurcated between hydroxyl (N13–H23N···O12) and methoxy oxygen atoms (N13–H23N···O13) forming stronger hydrogen bond with methoxy group (Table S4). There is a slight difference in strength of later hydrogen bond with hydroxyl oxygen atom (O12 and O22 denoted for both molecules) between methanol and ethanol derivative. Namely, this bond is remarkably longer in methanol derivative (3.310(3) and 3.497(3) Å *vs*. 3.345(2) and 3.691(2) Å) (Table S4).

The O4 oxygen atom of monohydrate **4b·H_2O** possesses (Fig. 14), multiple role in hydrogen bond formation interlinking molecules *via* hydrogen bonds with the carbonyl amide O1 atom, hydroxyl O2 atom and amine –NH group (Table S4). The hydroxyl O2 atom displays bifurcation between N2 and O4 atoms forming two hydrogen bonds: intramolecular O2–H12O···N2 and intermolecular O2–H12O···O4 (Table S4).

Water molecule does not participate into hydrogen bond formation with amine group, unlike alcohol solvent molecules in **4b·EtOH** and **4b·MeOH**. The amino N3 atom participates only in N3–H23N···O3 hydrogen bond formation with methoxy oxygen atom, while in **4b·EtOH** and **4b·MeOH**, except those hydrogen bonds, amine groups act as proton donors with hydroxyl oxygen and alcohol oxygen atoms. The hydrogen bonds of the C–H···O type which are different than in **4b·EtOH** and **4b·MeOH** derivatives are those with O4 atom and methoxy O3 atom (C4–H4···O3 and C8–H8···O4; Table S4).

The strong intramolecular hydrogen bond denoted as *S*(6) exists in **4c**. The intermolecular hydrogen bonds between amide nitrogen atoms and carbonyl oxygen atoms N11–H11N···O11 *i.e*. N21–H21N···O21 join symmetrically dependent molecules into *C*(4) 1D chains spreading along *c* axis (Fig. 14, Table S4). This crystal structure is only example, among described structures, exhibiting well-known *C*(4) supramolecular synthon between amide nitrogen atoms and carbonyl oxygen atoms.

The chains are interconnected *via* C–H···O intermolecular hydrogen bonds between C_{ar}-H groups and carbonyl amide oxygen atoms O11 and O21 as well as *via* N23–H43N···O12 hydrogen bond between amine nitrogen and hydroxyl oxygen atoms along *b* axis. The C–H···O bonds are formed only with amide oxygen atoms as proton acceptors. They are weak with the C···O distance range 3.300(5) – 3.586(5) Å. The oxygen atoms of methoxy groups do not participate into hydrogen bond formation.

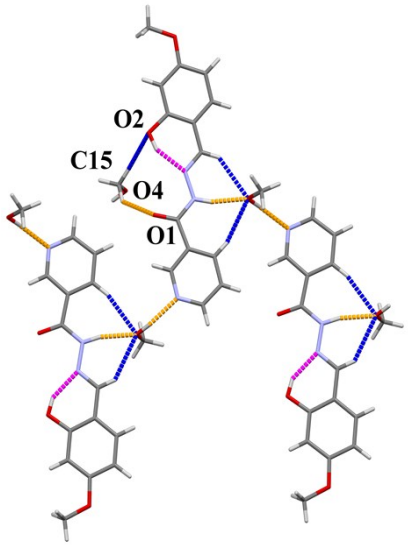

Fig. S15 Supramolecular assembling in **2c·MeOH**.

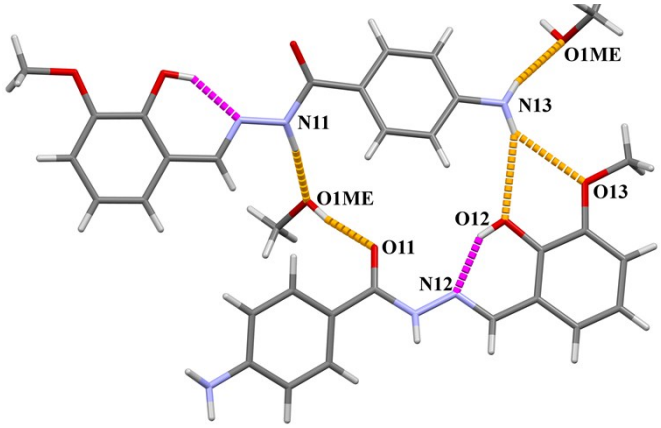

Fig. S16 Supramolecular assembling of **4b·MeOH** showing assembling of crystallographically dependent molecules *via* hydrogen bonds into sheets.

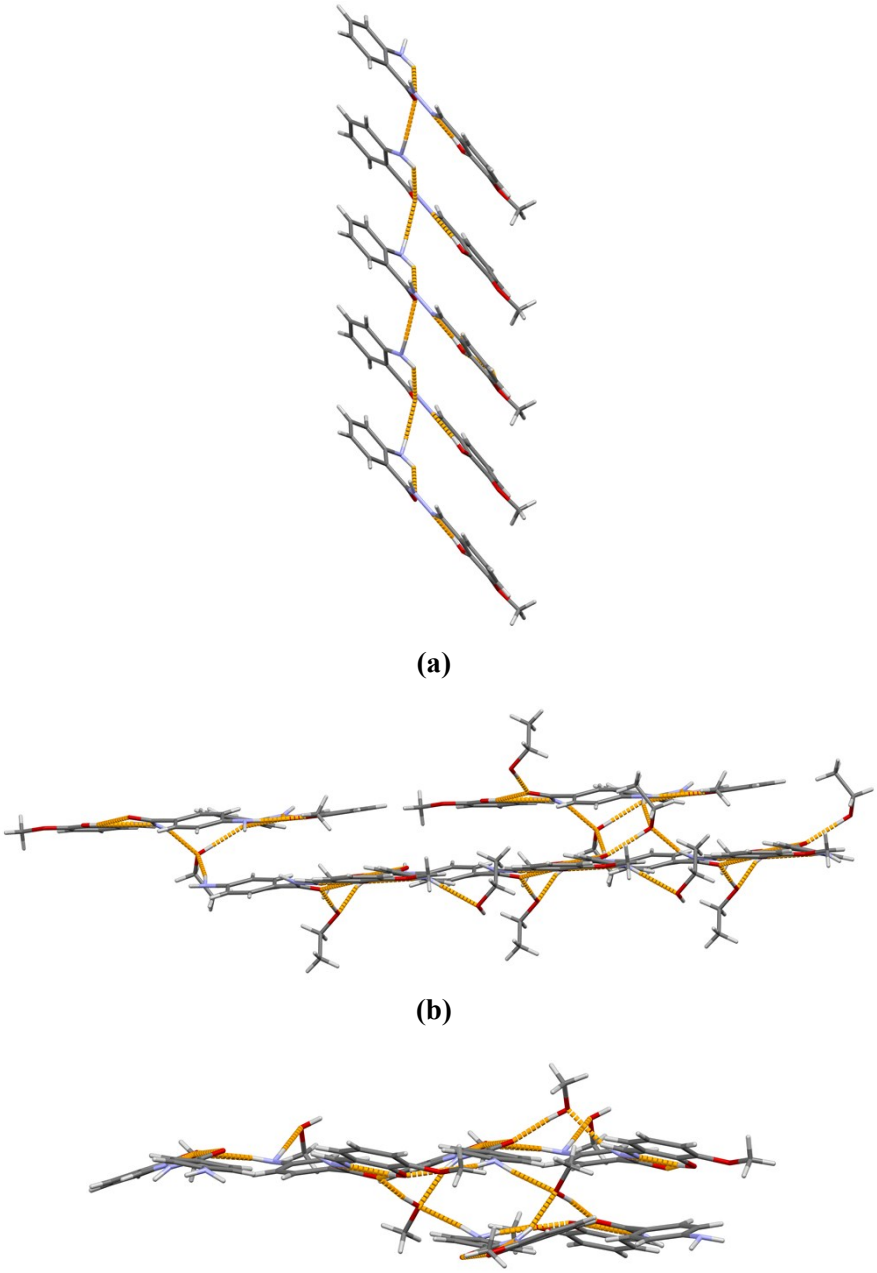

Fig. S17 Supramolecular assembling showing the bridging of sheets *via* hydrogen bonds with the amine N3 atom in (a) **3b** or solvent molecules of crystallization in (b) **4b·EtOH** and (c) **4b·MeOH**

Table S2 Selected bond lengths [Å] and angles [°] of the –C=N–NH–C(=O) fragment for compounds

Bond distances	**Nicotinehydrazide derivatives**		**Aminobenzydrazide derivatives**					
	2b·MeOH	**2c·MeOH**	**3b**	**4a**	**4b·EtOH**	**4b·MeOH**	**4b·H_2O**	**4c**
C1–O1	1.220(2)	1.222(2)	1.233(4)	1.225(4)	1.234(2) 1.238(2)	1.2396(18) 1.2401(18)	1.238 (7)	1.236(4) 1.234(5)
C1–N1	1.358(2)	1.353(2)	1.369(4)	1.363(4)	1.368(2) 1.367(2)	1.367(2) 1.372(2)	1.349 (7)	1.362(4) 1.359(5)
N1–N2	1.374(2)	1.383(2)	1.378(4)	1.385(3)	1.375(2) 1.374(2)	1.3765(17) 1.3713(17)	1.392 (6)	1.386(4) 1.378(4)
C7–N2 (C8–N2 in aminobenyhzdrazide derivatives)	1.273(2)	1.288(2)	1.284(4)	1.279(4)	1.284(2) 1.287(2)	1.291(2) 1.2816(19)	1.279 (7)	1.284(4) 1.273(5)
C9–O2 (C10–O2 in aminobenyhzdrazide derivatives)	1.353(2)	1.357(2)	1.365(4)	1.361(4)	1.361(2) 1.357(2)	1.3570(18) 1.3618(18)	1.358 (7)	1.370(4) 1.353(5)
Torsion angles								
τ: N2–N1–C1–C2	–179.86(16)	–177.47(11)	179.8(4)	–171.5(3)	178.80(15) –176.93(15)	175.39(12) 178.89(13)	–177.2 (5)	176.4(3) 170.9(4)
φ: C8–C7–N2–N1 (N1–N2–C8–C9 in aminobenyhzdrazide derivatives)	179.37(18)	–178.36(12)	178.9(4)	–179.4(3)	176.94(15) 177.10(15)	–177.51(13) –176.78(13)	–177.4 (5)	174.7(4) 175.8(4)

Table S3. Dihedral angles between phenyl rings planes

Compound	∠/°
nicotinic hydrazide derivatives	
2b·MeOH	6.1 (1)
2c·MeOH	2.2(1)
2 (or 4) aminohydrazide derivatives	
3b	27.5(2)
4a	22.5(2)
4b·EtOH	31.6(1) 19.1(1)
4b·MeOH	14.7(1) 27.7(1)
4b·H_2O	25.12(3)
4c	37.0(2) 33.0(2)

Table S4. Hydrogen bonds and interactions geometry (Å,°)

D−H···A	d(D−H)	d(H···A)	d(D···A)	<(DHA)	Symmetry code
2b·MeOH					
N1–H11N···O4	0.86 (2)	2.07 (2)	2.921 (2)	170 (2)	*x*+1, *y*, *z*
O2–H12O···N2	0.83 (2)	1.89 (2)	2.615 (2)	146 (2)	-
O4–H14O···N3	0.84 (2)	2.04 (2)	2.858 (2)	166 (2)	-
C4–H4···O3	0.93	2.57	3.433 (3)	154	-*x*+3/2, *y*+1/2, -*z*+3/2
C6–H6···O4	0.93	2.48	3.377 (3)	162	*x*+1, *y*, *z*
C7–H7···O4	0.93	2.64	3.412 (3)	140	*x*+1, *y*, *z*
C13–H13···O1	0.93	2.67	3.343(2)	131	*x*+1, *y*, *z*
C14–H14B···O1	0.96	2.63	3.182 (3)	117	*x*+1/2, -*y*-1/2, *z*-1/2
C15–H15B···O2	0.96	2.62	3.410 (3)	140	-*x*+1, -*y*, -*z*+1
2c·MeOH					
N1–H11N···O4	0.91 (2)	1.92 (2)	2.808 (2)	166.3 (17)	-*x*+1, *y*+1/2, -*z*+1/2
O2–H12O···N2	0.86 (2)	1.82 (2)	2.560 (2)	151.1 (18)	-
O4–H14O···N3	0.87 (2)	1.94 (2)	2.771 (2)	160.5 (17)	-
C6–H6···O4	0.95	2.41	3.328(2)	163	-x+1,+y+1/2,-z+1/2
C7–H7···O4	0.95	2.46	3.239 (2)	140	-*x*+1, *y*+1/2, -*z*+1/2
C10–H10···O2	0.95	2.55	3.411 (2)	151	-*x*+2, -*y*+1, -*z*+1
C15–H15A···O1	0.98	2.65	3.435 (2)	137	-*x*+1, -*y*+1, -*z*+1
C15–H15B···O2	0.98	2.54	3.478 (2)	160	-*x*+1, -*y*+1, -*z*+1
C15–H15C···O3	0.98	2.58	3.520 (2)	160	*x*-1, -*y*+3/2, *z*-1/2
3b					
N3–H13N···O1	0.88 (2)	2.12 (4)	2.755 (5)	129 (4)	-
N3–H23N···O1	0.87 (2)	2.17 (3)	3.012 (5)	165 (4)	*x*-1/2, -*y*-3/2, *z*
O2–H12O···N2	0.83 (2)	1.84 (3)	2.589 (5)	150 (4)	-
C8–H8···O1	0.93	2.76	3.599(5)	151	x,+y-1,+z
C13–H13···O2	0.93	2.64	3.216(4)	121	x,+y-1,+z
C13–H13···O3	0.93	2.69	3.602(4)	168	x,+y-1,+z
C14–H14···O2	0.93	2.60	3.193(4)	122	x,+y-1,+z
4a					
N1–H1N···O2	0.87 (2)	2.19 (2)	3.039 (3)	169 (3)	-x+1/2, y+1/2, z+1/2
N3–H23N···O1	0.87 (2)	2.34 (3)	3.129 (4)	152 (4)	-x+1, -y+2, z+1/2
O2–H22O···N2	0.83 (2)	1.90 (3)	2.652 (3)	150 (4)	-
C14–H14···O1	0.93	2.43	3.160(4)	135	-x+1/2, y-1/2, z+1/2
4b·EtOH					
O1–H10···O21	0.83 (2)	1.85 (2)	2.679 (2)	177 (2)	-x, y-1/2, -z+1/2
O2–H11···O11	0.83 (2)	1.84 (2)	2.666 (2)	175 (2)	-x+1, y-1/2, -z+1/2
N11–H11N···O2	0.91 (2)	1.93 (2)	2.814 (2)	161 (2)	x, y+1, z
O12–H12O···N12	0.90 (2)	1.79 (2)	2.573 (2)	144 (2)	-
N13–H13N···O2	0.89 (2)	2.36 (2)	3.245 (2)	170 (2)	-x+1, -y+1, -z

N21–H21N···O1	0.90 (2)	1.97 (2)	2.845 (2)	164 (2)	-
N13–H23N···O12	0.86 (2)	2.71 (2)	3.497 (3)	153 (2)	-x+1, y+1/2, -z+1/2
N13–H23N···O13	0.86 (2)	2.37 (2)	3.123 (2)	147 (2)	-x+1, y+1/2, -z+1/2
N23–H33N···O1	0.87 (1)	2.33 (2)	3.189 (2)	170 (2)	-x, -y+1, -z
N23–H43N···O22	0.88 (2)	2.49 (2)	3.310 (3)	156 (2)	-x, y-1/2, -z+1/2
N23–H43N···O23	0.88 (2)	2.45 (2)	3.187 (2)	141 (2)	-x, y-1/2, -z+1/2
O22–H22O···N22	0.84 (2)	1.83 (2)	2.595 (2)	152 (2)	-
C16–H16···O12	0.95	2.56	3.356 (3)	141	-x+1, y+1/2, -z+1/2
C24–H24···O22	0.95	2.50	3.312 (2)	143	-x, y-1/2, -z+1/2
C18–H18···O2	0.95	2.95	3.557 (2)	123	x, y+1, z
C115–H15C···O22	0.98	2.83	3.802 (3)	173	-
C215–H25C···O12	0.98	2.83	3.798 (3)	168	x, -y+3/2, z+1/2
4b·MeOH					
O12–H12O···N12	0.86 (1)	1.82 (2)	2.586 (2)	148 (2)	-
O1ME–H1···O11	0.86 (2)	1.81 (2)	2.663 (2)	169 (2)	-x+1, y+1/2
O2ME–H2···O21	0.86 (2)	1.78 (2)	2.637 (2)	172 (2)	-x, y+1/2, -z-1/2
N11–H12N···O1ME	0.89 (1)	2.00 (2)	2.867 (2)	165 (2)	x, y-1, z
N13–H13A···O12	0.89 (2)	2.53 (2)	3.345 (2)	152 (2)	-x+1, y-1/2, -z+1/2
N13–H13A···O13	0.89 (2)	2.48 (2)	3.257 (2)	146 (2)	-x+1, y-1/2, -z+1/2
N13–H13B···O1ME	0.89 (1)	2.28 (2)	3.150 (2)	167 (2)	-x+1, -y+1, -z
N21–H21N···O2ME	0.90 (1)	1.98 (2)	2.847 (2)	164 (2)	-
O22–H22···N22	0.87 (1)	1.77 (2)	2.570 (2)	153 (2)	-
N23–H23B···O2ME	0.89 (2)	2.26 (2)	3.142 (2)	169 (2)	-x, -y+1, -z-1
N23–H23A···O23	0.89 (2)	2.43 (2)	3.254 (2)	153 (2)	-x, y+1/2, -z-1/2
N23–H23A···O22	0.89 (2)	2.90(2)	3.691(2)	148(2)	-x,y+1/2,-z-1/2
C14–H14···O12	0.95	2.41	3.246 (2)	146	-x+1, y-1/2, -z+1/2
C24–H24···O22	0.95	2.52	3.361 (2)	148	-x, y+1/2, -z-1/2
C215–H25A···O12	0.98	2.64	3.591 (2)	163	-
4b·H_2O					
O4–H14O···O1	0.82 (3)	2.01 (3)	2.813 (7)	167 (9)	*x*, *y*, *z*+1
O4–H24O···O1	0.82 (3)	1.96 (3)	2.776 (7)	175 (8)	-
O2–H12O···N2	0.96 (6)	1.86 (6)	2.684 (6)	142 (5)	-
O2–H12O···O4	0.96 (6)	2.63 (6)	3.224 (7)	120 (5)	-
N1–H11N···O4	0.86 (3)	2.02 (3)	2.865 (7)	165 (7)	-*x*+3/2, *y*-1/2, *z*-1/2
N3–H23N···O3	0.85 (3)	2.51 (6)	3.201 (8)	140 (7)	-*x*+3/2, *y*-1/2, *z*-3/2
C6–H6···O3	0.93	2.63	3.371 (8)	137	-*x*+3/2, *y*-1/2, *z*-3/2

C8–H8···O1	0.93	2.89	3.771 (8)	159	-*x*+3/2, *y*-1/2, *z*+1/2
C8–H8···O4	0.93	2.56	3.314 (8)	138	-*x*+3/2, *y*-1/2, *z*-1/2
C15—H15C···O2	0.96	2.89	3.676 (9)	140	*x*, *y*, *z*+1
4c					
N11–H11N···O11	0.85 (2)	2.01 (2)	2.825 (4)	159 (3)	x, -y, z+1/2
O12–H12O···N12	0.86 (2)	1.85 (4)	2.591 (5)	143 (5)	-
N21–H21N···O21	0.88 (4)	2.16 (4)	3.037 (4)	172 (4)	x, -y+1, z+1/2
O22–H22O···N22	0.83 (2)	1.87 (3)	2.619 (4)	149 (4)	-
N23–H43N···O12	0.86 (2)	2.53 (3)	3.323 (6)	154 (4)	x-1, -y+1, z+1/2
C16–H16···O21	0.93	2.67	3.585 (6)	167	x+1, y-1, z
C26–H26···O11	0.93	2.64	3.405 (6)	140	x-1, -y+1, z+1/2
C18–H18···O11	0.93	2.54	3.300 (5)	139	x, -y, z+1/2
C28–H28···O21	0.93	2.81	3.586 (5)	141	x, -y+1, z+1/2
C215–H15D···N12	0.96	2.83	3.577 (7)	136	-

8. NMR spectroscopy

Table S5 ^{1}H and ^{13}C chemical shifts (ppm) of **1a**, **1b** and **1c**.

Atom	**1a**		**1b**		**1c**	
	δ / ppm (^{1}H)	δ / ppm (^{13}C)	δ / ppm (^{1}H)	δ / ppm (^{13}C)	δ / ppm (^{1}H)	δ / ppm (^{13}C)
1	8.69	149.44	8.70	149.27	8.58	150.01
4	–	161.81	–	161.79	–	161.52
5	–	140.45	–	140.50	–	140.50
6	7.85	121.98	7.85	121.98	7.84	121.92
7	8.81	150.97	8.80	150.86	8.80	150.83
8	–	–	–	–	–	–
9	8.81	150.87	8.80	150.86	8.80	150.83
10	7.85	121.98	7.85	121.98	7.84	121.92
11	–	119.17	–	119.46	–	112.16
12	–	157.95	–	147.64	–	159.90
13	6.95	116.92	–	148.46	6.54	101.62
14	7.32	132.22	7.06	114.44	–	162.80
15	6.93	119.91	6.88	119.62	6.51	107.09
16	7.61	129.68	7.21	120.87	7.49	131.47
OH	11.08	–	10.69	–	11.42	–
NH	12.29	–	12.26	–	12.19	–
OMe	–	–	3.83	56.32	3.78	55.81

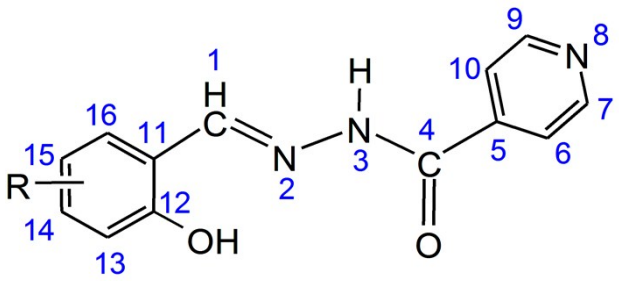

Scheme S4. The structural formula of **1a**-**1c** with the NMR numbering scheme

Table S6 ^{1}H and ^{13}C chemical shifts (ppm) of **2a**, **2b** and **2c**.

Atom	**2a**		**2b**		**2c**	
	δ / ppm (^{1}H)	δ / ppm (^{13}C)	δ / ppm (^{1}H)	δ / ppm (^{13}C)	δ / ppm (^{1}H)	δ / ppm (^{13}C)
1	8.66	149.11	8.67	148.89	8.56	149.62
4	–	161.91	–	161.89	–	161.66
5	–	129.17	–	129.21	–	129.24
6	9.10	149.03	9.09	149.10	9.08	149.04
7	–	–	–	–	–	–
8	8.79	152.93	8.78	152.81	8.78	152.85
9	7.58	124.13	7.59	124.12	7.59	124.12
10	8.28	135.94	8.28	135.93	8.25	135.87
11	–	119.15	–	119.43	–	112.18
12	–	157.93	–	147.62	–	159.91
13	6.95	116.91	–	148.44	6.51	101.64
14	7.32	132.09	7.05	114.37	–	162.72
15	6.93	119.88	6.88	119.59	6.54	107.05
16	7.59	129.79	7.20	121.02	7.47	131.54
OH	11.15	–	10.79	–	11.49	–
NH	12.25	–	12.22	–	12.15	–
OMe	–	–	3.82	56.31	3.78	55.81

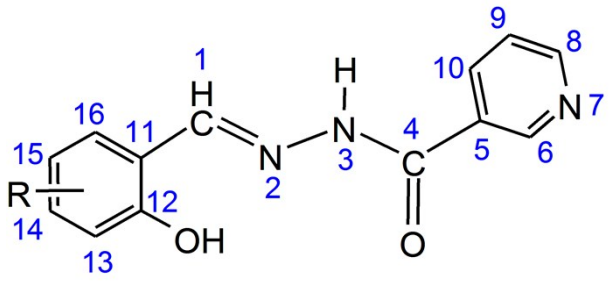

Scheme S5. The structural formula of **2a**-**2c** with the NMR numbering scheme

Table S7 ^{1}H and ^{13}C chemical shifts (ppm) of **3a**, **3b** and **3c**.

Atom	**3a**		**3b**		**3c**	
	δ / ppm (^{1}H)	δ / ppm (^{13}C)	δ / ppm (^{1}H)	δ / ppm (^{13}C)	δ / ppm (^{1}H)	δ / ppm (^{13}C)
1	8.60	148.22	8.59	148.09	8.49	148.65
4	–	165.48	–	165.45	–	165.42
5	–	112.90	–	112.97	–	113.08
6	–	150.81	–	150.79	–	150.71
7	6.80	117.01	6.78	116.98	6.77	116.95
8	7.23	133.06	7.22	133.03	7.21	132.92
9	6.60	119.76	6.59	115.09	6.58	115.08
10	7.62	130.23	7.60	128.73	7.58	128.66
11	–	119.14	–	119.35	–	112.29
12	–	157.97	–	147.66	–	159.91
13	6.95	116.90	–	148.40	6.50	101.67
14	7.30	131.60	7.03	114.19	–	162.36
15	6.93	119.76	6.86	119.43	6.52	106.86
16	7.50	130.23	7.10	121.57	7.38	131.72
OH	11.53	–	11.24	–	11.82	–
NH	11.91	–	11.86	–	11.77	–
NH_2	6.51	–	6.48	–	6.46	–
OMe	–	–	3.82	56.29	3.78	55.78

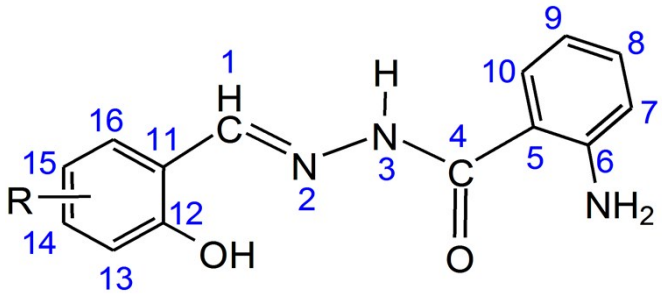

Scheme S6. The structural formula of **3a-3c** with the NMR numbering scheme

Table S8 ^{1}H and ^{13}C chemical shifts (ppm) of **4a**, **4b** and **4c**.

Atom	**4a**		**4b**		**4c**	
	δ / ppm (^{1}H)	δ / ppm (^{13}C)	δ / ppm (^{1}H)	δ / ppm (^{13}C)	δ / ppm (^{1}H)	δ / ppm (^{13}C)
1	8.56	147.37	8.56	147.32	8.48	147.84
4	–	163.13	–	163.09	–	162.94
5	–	119.23	–	119.42	–	119.35
6	7.70	129.89	7.69	129.88	7.67	129.77
7	6.62	113.13	6.61	113.12	6.61	113.12
8	–	153.03	–	153.01	–	152.92
9	7.70	113.13	6.61	113.112	6.61	113.12
10	–	129.89	7.69	129.88	7.67	129.77
11	–	119.19	–	119.23	–	112.40
12	6.93	157.88	–	147.60	–	159.83
13	6.29	116.85	–	148.38	6.50	101.67
14	6.91	131.38	7.00	114.04	–	162.18
15	7.47	119.71	6.85	119.37	6.52	106.76
16	7.47	130.14	7.02	121.59	7.36	131.61
OH	11.56	–	11.33	–	11.88	–
NH	11.76	–	11.71	–	11.62	–
NH_2	5.84	–	5.83	–	5.81	–
OMe	–	–	3.81	56.28	3.78	55.76

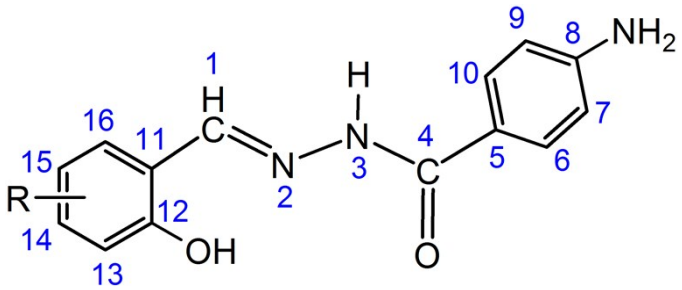

Scheme S7**.** The structural formula of **4a**-**4c** with the NMR numbering scheme